NAVAL POSTGRADUATE SCHOOL

MONTEREY, CALIFORNIA

THESIS

NOSE FAIRING MODELING AND SIMULATION TO SUPPORT TRIDENT II D5 LIFECYCLE EXTENSION

by

Robert D. Blanchard

September 2013

Thesis Advisor: Ramesh Kolar
Second Reader: Fotis Papoulias

Approved for public release; distribution is unlimited

THIS PAGE INTENTIONALLY LEFT BLANK

REPORT DOCUMENTATION PAGE		*Form Approved OMB No. 0704-0188*

Public reporting burden for this collection of information is estimated to average 1 hour per response, including the time for reviewing instruction, searching existing data sources, gathering and maintaining the data needed, and completing and reviewing the collection of information. Send comments regarding this burden estimate or any other aspect of this collection of information, including suggestions for reducing this burden, to Washington headquarters Services, Directorate for Information Operations and Reports, 1215 Jefferson Davis Highway, Suite 1204, Arlington, VA 22202-4302, and to the Office of Management and Budget, Paperwork Reduction Project (0704-0188) Washington DC 20503.

1. AGENCY USE ONLY *(Leave blank)*	**2. REPORT DATE** September 2013	**3. REPORT TYPE AND DATES COVERED** Master's Thesis
4. TITLE AND SUBTITLE NOSE FAIRING MODELING AND SIMULATION TO SUPPORT TRIDENT II D5 LIFECYCLE EXTENSION		**5. FUNDING NUMBERS**
6. AUTHOR(S) Robert D. Blanchard		

7. PERFORMING ORGANIZATION NAME(S) AND ADDRESS(ES)
  Naval Postgraduate School
  Monterey, CA 93943-5000
		8. PERFORMING ORGANIZATION REPORT NUMBER

9. SPONSORING /MONITORING AGENCY NAME(S) AND ADDRESS(ES) N/A		**10. SPONSORING/MONITORING AGENCY REPORT NUMBER**

11. SUPPLEMENTARY NOTES The views expressed in this thesis are those of the author and do not reflect the official policy or position of the Department of Defense or the U.S. government. IRB Protocol number _____N/A_____.

12a. DISTRIBUTION / AVAILABILITY STATEMENT Approved for public release; distribution is unlimited.	**12b. DISTRIBUTION CODE** A

13. ABSTRACT (maximum 200 words)

The objective of this thesis is to evaluate a modeling and simulation tool for the analysis of the Trident II D5 missile nose fairing to determine the limitations of serviceability through the extended service life of the D5 missile. The benefit of this analysis is a means to evaluate and manage the remaining nose fairing supply and serve as a baseline for future production of nose fairings.

Constructed of a Sitka spruce and fiberglass laminate, the nose fairing is designed as the lifting point of the missile for submarine onloads and offloads and supports the entire weight of the missile. A computer model of the nose fairing was used to evaluate the nose fairing under tensile and compressive loading conditions to simulate the lifting evolution and closure segment impact at time of launch. Changes in the material properties of the model allow for a simulation of aging in the nose fairing to estimate the performance degradation over time, as well as exploration of the applicability of new materials to any future design of nose fairings.

14. SUBJECT TERMS Trident II D5, composites, nose fairing, ANSYS, modeling and simulation			**15. NUMBER OF PAGES** 61
			16. PRICE CODE
17. SECURITY CLASSIFICATION OF REPORT Unclassified	**18. SECURITY CLASSIFICATION OF THIS PAGE** Unclassified	**19. SECURITY CLASSIFICATION OF ABSTRACT** Unclassified	**20. LIMITATION OF ABSTRACT** UU

NSN 7540-01-280-5500

Standard Form 298 (Rev. 2-89)
Prescribed by ANSI Std. 239-18

THIS PAGE INTENTIONALLY LEFT BLANK

NOSE FAIRING MODELING AND SIMULATION TO SUPPORT TRIDENT II D5 LIFECYCLE EXTENSION

Robert D. Blanchard
Lieutenant, United States Navy
B.S., Texas A&M University, 2003

Submitted in partial fulfillment of the
requirements for the degree of

MASTER OF SCIENCE IN MECHANICAL ENGINEERING

from the

**NAVAL POSTGRADUATE SCHOOL
September 2013**

Author: Robert D. Blanchard

Approved by: Ramesh Kolar
                 Thesis Advisor

                 Fotis Papoulias
                 Second Reader

                 Knox Millsaps
                 Chair, Department of Mechanical and Aerospace Engineering

THIS PAGE INTENTIONALLY LEFT BLANK

ABSTRACT

The objective of this thesis is to evaluate a modeling and simulation tool for the analysis of the Trident II D5 missile nose fairing to determine the limitations of serviceability through the extended service life of the D5 missile. The benefit of this analysis is a means to evaluate and manage the remaining nose fairing supply and serve as a baseline for future production of nose fairings.

Constructed of a Sitka spruce and fiberglass laminate, the nose fairing is designed as the lifting point of the missile for submarine onloads and offloads and supports the entire weight of the missile. A computer model of the nose fairing was used to evaluate the nose fairing under tensile and compressive loading conditions to simulate the lifting evolution and closure segment impact at time of launch. Changes in the material properties of the model allow for a simulation of aging in the nose fairing to estimate the performance degradation over time, as well as exploration of the applicability of new materials to any future design of nose fairings.

THIS PAGE INTENTIONALLY LEFT BLANK

TABLE OF CONTENTS

LIST OF FIGURES

THIS PAGE INTENTIONALLY LEFT BLANK

LIST OF TABLES

THIS PAGE INTENTIONALLY LEFT BLANK

LIST OF ACRONYMS AND ABBREVIATIONS

ASTM   American Society for Testing and Materials

FY   Fiscal Year

HMS   Her/His Majesty's Ship (UK)

LE   Life Extension

PBCS   Post Boost Control System

RV   Reentry Vehicle

SLBM   Submarine Launched Ballistic Missile

SSBN   Ship, Submersible, Ballistic, Nuclear

USS   United States Ship

VV&A   Verification, Validation, and Accreditation

THIS PAGE INTENTIONALLY LEFT BLANK

ACKNOWLEDGMENTS

THIS PAGE INTENTIONALLY LEFT BLANK

I.   INTRODUCTION

A.   OBJECTIVE

The objective of this thesis is to evaluate a modeling and simulation tool for the continued use of the Trident II D5 missile nose fairing. Evaluating the design and materials for engineering projects has often included destructive tests that are costly in both time and money. With the increase in computer processing capabilities and the proliferation of engineering analysis software there is an opportunity to reduce the need for these expensive test methods. Appropriately constructed computer models can be programmed to simulate a wide range of conditions (tensile stress, compression, fluid flow, etc.) and numerically analyzed based on the intended service environment. While it will not eliminate the need for destructive testing, modeling and simulation provides a valuable non–destructive evaluation tool for engineers. For the purpose of this thesis, all information used to develop the models for the nose fairing is based on open source data and most values and dimensions are notional.

B.   BACKGROUND

1.   Trident II D5 Missile

As the latest Submarine Launched Ballistic Missile (SLBM) in the arsenal of the United States and Great Britain, the Trident II D5 has been in service since 1990 [1, 2]. The D5 is deployed on the HMS Vanguard class and the USS OHIO class submarines [1, 2] as the most survivable leg of the nuclear deterrent triad [3]. Continuing the legacy of the U.S. SLBM program into the sixth generation [1], D5 provided increased capability over its predecessor the Trident I C4 [4]. Figure 1 and Table 1 show size and capability comparisons of missiles starting with the first generation Polaris A1.

A three stage, solid propellant missile, the D5 uses inertial and stellar guidance technology [4]. The three rocket motor stages are nearly 26 feet, eight feet, and 10 feet long respectively, weighing in at about 65,000, 19,000 and 4,000 pounds each [4]. First and second stage motors are the full missile diameter of almost seven feet, while the third stage is a slimmer two and a half feet wide to fit inside the Post–Boost Control System

(PBCS) of the equipment section of the missile. With a length of 44 feet and weighing about 130,000 lbs., the D5 will reach a speed in excess of 20,000 feet per second within two minutes of leaving the submarine after the third stage motor ignites [4].
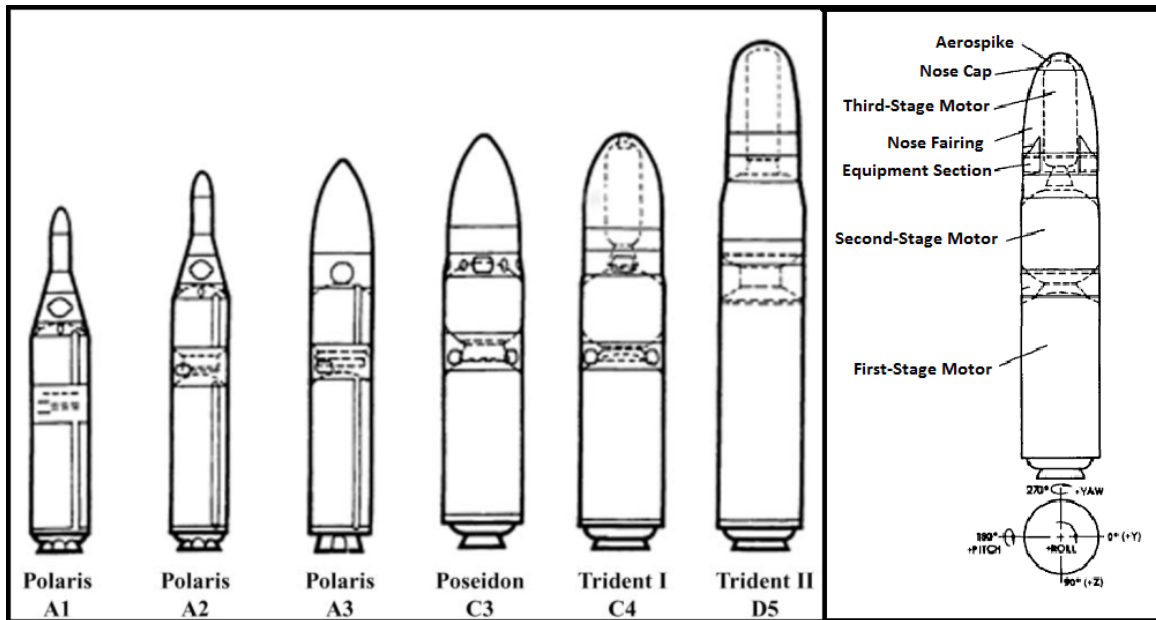
Figure 1.   Size Comparison of the Six Generations of SLBM Missiles (After [5])

	POLARIS (A1)	POLARIS (A2)	POLARIS (A3)	POSEIDON (C3)	TRIDENT I (C4)	TRIDENT II (D5)
Length	28 feet	31 feet	32 feet	34 feet	34 feet	44 feet
Diameter	54 inches	54 inches	54 inches	74 inches	74 inches	83 inches
Weight	28,000 pounds	32,500 pounds	35,700 pounds	64,000 pounds	73,000 pounds	130,000 pounds (approx)
Powered Stages	2	2	2	2	3	3
Motor Case Materials	1st Stage - Low alloy steel 2nd Stage - Low alloy steel	1st Stage - Steel 2nd Stage - Glass Fiber	1st Stage - Glass Fiber[1] 2nd Stage - Glass Fiber[1]	1st Stage - Glass Fiber 2nd Stage - Glass Fiber	All 3 Stages Kevlar/Epoxy	1st Stage - Graphite/Epoxy 2nd Stage - Graphite/Epoxy 3rd Stage - Kevlar/Epoxy
Nozzles	4, each stage	4, each stage	4, each stage	1, each stage	1, each stage	1, each stage
Controls	Jetevators	1st Stage - Jetevators 2nd Stage - Rotating Nozzles	1st Stage - Rotating Nozzles[2] 2nd Stage - Fluid Injection[2]	Single Movable Nozzle Actuated by a Gas Generator	Single Movable Nozzle Actuated by a Gas Generator	Single Movable Nozzle Actuated by a Gas Generator
Propellant	Solid	Solid	Solid 1st Stage - Composite	Solid 1st Stage - Composite	Solid Cross-Linked Double Base	Solid Nitrate Ester Plasticized Polyethylene Glycol
Guidance	All Inertial	All Inertial	All Inertial	All Inertial	Stellar and Inertial	Stellar and Inertial
Range (nominal)	1,200 NM (1,380 SM)	1,500 NM (1,730 SM)	2,500 NM (2,880 SM)	2,500 NM (2,880 SM)	4,000 NM (4,600 SM)	> 4,000 NM (4,600 SM)
Warheads	Nuclear	Nuclear	Nuclear	Nuclear	Nuclear	Nuclear

POLARIS, POSEIDON, AND TRIDENT MISSILES (A1, A2, A3, C3, C4, D5) DESCRIPTIVE SUMMARY COMPARISON

NOTES: [1] First large ballistic missile to use glass motor case for all stages. (Small glass-fiber motor case had previously flown in Vanguard Program. POLARIS was first large glass-fiber rocket motor case.)

[2] Devised and first flown by Navy in POLARIS development program.

Table 1.   SLBM Missile Specifications Comparison (From [6])

Several technological advances contribute to the capability of the D5. Lighter, stronger materials [1] and a significantly larger first stage motor [4] give the D5 a larger payload capacity than previous designs. To garner about 50 percent reduction in drag [1] the D5 employs the telescoping aerospike, developed for the C4, during first stage burn [4]. Combined with the additional thrust this increased the missile's range to greater than 4,000 nautical miles [1].

2. Nose Fairing

An interesting engineering challenge and important part of the missile is the nose fairing. At the top of the missile, the nose fairing is attached to the equipment section of the missile and encloses the PBCS, reentry vehicle (RV) mounting platform, and third stage rocket motor [4]. Fixed to the forward end of the nose fairing is the nose cap which houses the aerospike. The attachment points to the nose fairing are solid machined aluminum rings. These rings are integrated into the shell of the nose fairing via aluminum sheets laminated into the ends of the Sitka spruce and fiberglass sheets making up the major body of the nose fairing.

This Sitka spruce laminate shell composition is one that was developed for the Poseidon missile and has been passed down to the Trident designs to address some unique operational requirements the nose fairing must meet. When the missile is launched from the submarine, the nose fairing is subjected to a compressive axial load as it breeches the segmented missile tube closure. Following departure from the closure, the missile travels through the layer of seawater above the submarine and endures new stresses due to the surface broach as it leaves the water. In addition to these launch transients and its role as the transitional aerodynamic component from the aerospike and nose cap to the main body of the missile, the nose fairing is designed to lift the missile into and out of the submarine. The entire weight of the missile is suspended during these operations by means of a special missile lifting fixture that fastens to the nose fairing at the aluminum ring where the nose cap is normally attached.

These loads might suggest that the nose fairing should be constructed of some form of metal that would easily handle the burden. One final requirement though prohibits the use of metals. When the missile is equipped for test flights telemetry equipment is mounted in the equipment section of the missile. Transmission of the telemetry data must pass through the nose fairing to be received at the monitoring stations. Any materials that are radio frequency (RF) inhibiting (such as metals) must be excluded from those used to build the nose fairing shell.

3.   Life Extension

Originally, the service life of the OHIO class submarines was to be 30 years. This meant a timeline for end of service for the class to begin around fiscal year (FY) 2014. As this time neared, the first four submarines in the class were converted to Guided Missile platforms leaving 14 SSBNs in the fleet [4]. However, to continue to meet the nuclear deterrent mission objectives, the service life for the remaining subs was extended to 45 years [7]. To support the submarine extension a D5 life extension (LE) was required.

Along with the need for additional test missiles to support the program's annual reliability test requirements [7], the D5 LE meant that there would be a need to produce additional replacement parts for those that would reach the end of serviceability before the program. Original D5 procurement orders called for 425 missiles in 18 years, beginning in 1989. For the D5 LE a contract was signed that scheduled delivery of an additional 108 missiles in six years beginning in 2011 [7].

As part of the acquisition process for the TRIDENT II D5, nose fairings were procured with the objective of providing a supply sufficient for the original life of the program. In early 2011 the final nose fairing for the original acquisition was produced and delivered. This end of production means that the nose fairings in service or storage now have no planned replacements.

THIS PAGE INTENTIONALLY LEFT BLANK

II.   LITERATURE REVIEW

A.   COMPOSITES

1.   What is a Composite?

Composites are natural or man–made materials that combine two or more materials into a single material that has the benefits of the desirable properties of the constituent materials [8, 9]. The use of composite materials has become a common practice to overcome engineering problems that have proven to be too difficult to solve with conventional materials. Despite what many think about them, composites are not a new engineering phenomenon. Composites have been used to provide better structural and material properties for a long time. Examples are readily identified in many common items. Concrete, a mixture of sand and cementing materials, (more recently) combined with steel bars [9], and bricks, mud or clay mixed with straw or other fibrous material [10], are examples of composites that have been around for many centuries. New, purpose built composites have also been developed from modern engineered materials, such as carbon fiber and Kevlar, to address increasingly difficult engineering problems. These composite materials are designed to perform better than conventional materials in a variety of areas such as stiffness, strength to weight, fatigue life and corrosion resistance to name a few [8].

2.   Composite Mechanics versus Conventional Materials and the Generalized Hooke's Law

In analysis of conventional materials (such as metals) the properties used to describe and evaluate how the material is affected by outside actions or forces are omni– directional. These properties are therefore isotropic within the material. In addition, these material properties are generally the same regardless of the physical position in a material, making them homogenous as well [8]. Most commonly, material evaluation is done using the methods of solid mechanics, where relationships between stress and strain in a material are calculated for the force (stress) exerted on the material. The main properties (elastic material constants) used to describe these homogenous, isotropic

materials are measures of the material's elasticity (the elastic modulus (E)), the shear modulus (G, also known as the modulus of rigidity), and the Poisson's ratio (ν) that describes the transverse strain perpendicular to an axial strain [11].

A relationship for the stress and strain in one dimension of an isotropic material is given by Hooke's law, where the stress is proportional to the elastic modulus and Poisson's ratio [12]. For two or three dimensional stress states only two independent elastic material constants are needed to write the Hooke's Law relationships as seen in the following taken from [12]:

For example, a plane state stress state is governed by the following relations:

$$\sigma_1 = (\varepsilon_1 + \nu\varepsilon_2)\frac{E}{1-\nu^2}$$

$$\sigma_2 = (\varepsilon_2 + \nu\varepsilon_1)\frac{E}{1-\nu^2} \qquad (2\text{-}16)$$

$$\tau12 = (\gamma12)G$$

Two independent material elastic constants appear in equation (2-16). The third elastic constant, shear modulus, G, is a function of the other two elastic constants, E and ν. This relationship is given by:

$$G = E / 2(1+\nu)$$

Unlike conventional materials, the properties of composites are often dependent on the physical location (heterogeneous) and the relative orientation (anisotropic) within the material [8]. This complex nature of composite material properties means they will react differently to external actions than isotropic materials. Figure 2, from Ochoa Reddy [8] shows how an anisotropic material differs in deformation from an isotropic material. It can be seen from the figure that a normal stress or strain on an anisotropic body results in both normal and shear stresses and strains, respectively [8].
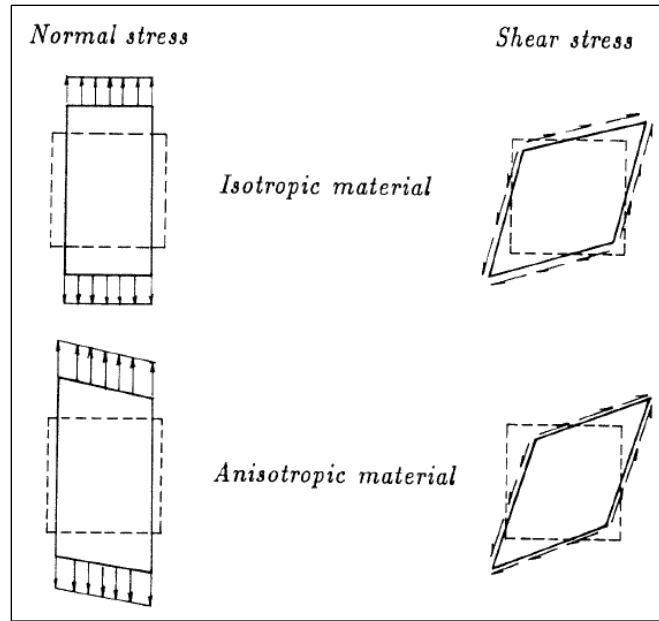
Figure 2.   Deformation of Isotropic and Anisotropic Material Elements Subjected to Normal and Shear Stresses (Dashed Line is Undeformed Geometry) (From [8])
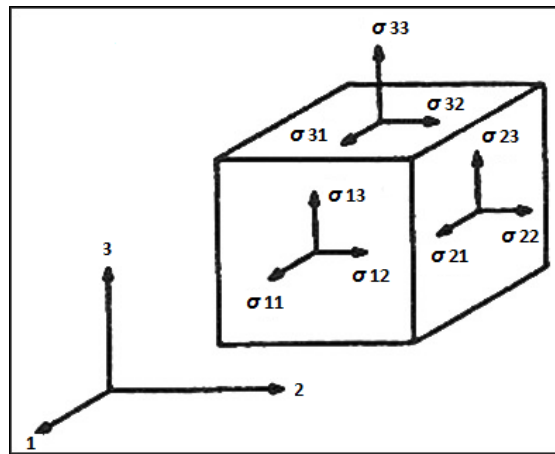
Figure 3.   Three Dimensional Stress State (From [12])

The difference from isotropic materials means that conventional analysis of composite materials is not readily applicable. To determine the resultant stresses and strains for a composite, the material orientation relative to the applied stress must be taken into account. Hooke's Law for an anisotropic material in a three dimensional state of stress as in Figure 3 demonstrates the most general case, with 21 independent elastic constants [12] and illustrates the complexity that a composite can present for analysis.

9

From Ochoa and Reddy [8] the tensor form of the generalized Hooke's Law to relate stress and strain for an anisotropic material is given by Equation (1):

$$\sigma_{ij} = c_{ijkl}\varepsilon_{kl}$$

(1)

Using this formula, the elastic coefficient matrix of 81 constants can be written as in Equation (2), as modified from Halpin [12].

$$
\begin{Bmatrix} \sigma_{11} \\ \sigma_{22} \\ \sigma_{33} \\ \sigma_{23} \\ \sigma_{31} \\ \sigma_{12} \\ \sigma_{32} \\ \sigma_{13} \\ \sigma_{21} \end{Bmatrix} =
\begin{bmatrix} C_{1111} & C_{1122} & C_{1133} & C_{1123} & C_{1131} & C_{1112} & C_{1132} & C_{1113} & C_{1121} \\ C_{2211} & C_{2222} & C_{2233} & C_{2223} & C_{2231} & C_{2212} & C_{2232} & C_{2213} & C_{2221} \\ & & & & & & & & \\ & & & & & & & & \\ & & & & & & & & \\ & & & & & & & & \\ & & & & & & & & \\ & & & & & & & & \\ C_{2111} & C_{2122} & C_{2133} & C_{2123} & C_{2131} & C_{2112} & C_{2132} & C_{2113} & C_{2121} \end{bmatrix}
\begin{Bmatrix} \varepsilon_{11} \\ \varepsilon_{22} \\ \varepsilon_{33} \\ \varepsilon_{23} \\ \varepsilon_{31} \\ \varepsilon_{12} \\ \varepsilon_{32} \\ \varepsilon_{13} \\ \varepsilon_{21} \end{Bmatrix}
$$

(2)

This matrix is referred to as the material stiffness matrix and it gives the stress-strain relation for a material. Its inverse, known as the compliance matrix, gives the strain–stress relation [12]. Fortunately, not all composites are anisotropic. Symmetry of some composite forms allows the coefficient and compliance matrices to be simplified and makes them easier to work with for analysis. It is shown by Halpin [12] that the stiffness and compliance matrices must be symmetric, reducing the 81 constants to the previously mentioned 21 independent constants. With this and use of an abbreviation of the proper tensor form the stiffness matrix can be written as Equation (3), modified from Ochoa and Reddy [8].

$$
\begin{Bmatrix} \sigma_1 \\ \sigma_2 \\ \sigma_3 \\ \sigma_4 \\ \sigma_5 \\ \sigma_6 \end{Bmatrix} =
\begin{bmatrix} C_{11} & C_{12} & C_{13} & C_{14} & C_{15} & C_{16} \\ & C_{22} & C_{23} & C_{24} & C_{25} & C_{26} \\ & & C_{33} & C_{34} & C_{35} & C_{36} \\ & & & C_{44} & C_{45} & C_{46} \\ & & & & C_{55} & C_{56} \\ & sym. & & & & C_{66} \end{bmatrix}
\begin{Bmatrix} \varepsilon_1 \\ \varepsilon_2 \\ \varepsilon_3 \\ \varepsilon_4 \\ \varepsilon_5 \\ \varepsilon_6 \end{Bmatrix}
$$

(3)

where,

$$\sigma_1 = \sigma_{11}, \sigma_2 = \sigma_{22}, \sigma_3 = \sigma_{33}, \sigma_4 = \sigma_{23}, \sigma_5 = \sigma_{13}, \sigma_6 = \sigma_{12}$$
$$\varepsilon_1 = \varepsilon_{11}, \varepsilon_2 = \varepsilon_{22}, \varepsilon_3 = \varepsilon_{33}, \varepsilon_4 = 2\varepsilon_{23}, \varepsilon_5 = 2\varepsilon_{13}, \varepsilon_6 = 2\varepsilon_{12}$$

3. Orthotropic Composites

A material can be anisotropic and still have some material properties that are orientation dependent to a degree. These special cases have material symmetry that allows for further simplification of the stiffness and compliance matrices by reducing the number of independent constants. Ochoa and Reddy describe this property as follows:

> When the elastic coefficients at a point have the same values for every pair of coordinate systems which are mirror images of each other in a certain plane, that plane is called a plane of elastic symmetry for the material at that point. Materials with one plane of symmetry are called monoclinic materials, and the number of elastic coefficients for such materials reduces to 13 [8].

Of particular interest in composites is the case of materials with three mutually perpendicular (orthogonal) planes of elastic symmetry. These materials are known as orthotropic and have only nine independent constants. From [8], Equation (4) shows the simplified stiffness matrix for an orthotropic material.

$$
\begin{Bmatrix} \sigma_1 \\ \sigma_2 \\ \sigma_3 \\ \sigma_4 \\ \sigma_5 \\ \sigma_6 \end{Bmatrix} = \begin{vmatrix} C_{11} & C_{12} & C_{13} & 0 & 0 & 0 \\ & C_{22} & C_{23} & 0 & 0 & 0 \\ & & C_{33} & 0 & 0 & 0 \\ & & & C_{44} & 0 & 0 \\ & & & & C_{55} & 0 \\ & & & & & C_{66} \end{vmatrix} \begin{Bmatrix} \varepsilon_1 \\ \varepsilon_2 \\ \varepsilon_3 \\ \varepsilon_4 \\ \varepsilon_5 \\ \varepsilon_6 \end{Bmatrix}
\tag{4}
$$

B. LAMINATE PLATE THEORY

The complex interactions of the materials within a composite (as illustrated in the previous section) can make analysis of a composite structure very difficult. Fortunately there are assumptions that can be made to simplify the analysis of some composite forms. The nose fairing is built using one of these forms. Constructed as a sheet of multiple layers called lamina bonded together, the nose fairing is a laminate of alternating spruce and fiberglass.

Due to the thickness of a laminate being dimensionally much smaller than the length and width it resembles a plate. Using this and making assumptions about deformation of the laminate in the z–direction (through the thickness of the material) an

extension of plate theory can be utilized for analysis of laminates [8]. The three basic assumptions are described in Ochoa and Reddy [8] from the Kirchhoff–Love hypothesis such that "straight lines perpendicular to the midplane before deformation remain (1) straight, (2) inextensible, and (3) normal to the midsurface after deformation."

These few assumptions lead to being able to neglect transverse strain with respect to the direction of thickness. Further work and application to particular laminate construction (specifically orthotropic laminate) shows that the related stresses will also be negligible. The results an artificial assumption of "infinite" rigidity in the transverse direction that means the laminate resembles a plate when subjected to inplane forces and strains [8].

1.   ABD Matrix

Using laminate plate theory requires that the full thickness of the laminate in question be evaluated as a continuous layer. Without some method to resolve the individual lamina into a single plate this would be very difficult. Using the midplane geometry of the laminate construction and equations defining the stresses acting on individual lamina a mathematical description of the relationships between the laminate's force and moment system, the midplane strains, and the plate curvature can be derived. These are known as the laminate constitutive equations and can be written in a simplified form termed the ABD matrix. There can be found in both the Halpin [12] and Ochoa–Redding [8] texts great descriptions of the ABD derivation. For the benefit of general understanding, how the matrix is found is briefly described here.

Using the Equations (5) and (6) for stress state in the kth ply of a laminate from Halpin [12] Equations (3-16) and (3-17),

$$\begin{bmatrix} \sigma_x \\ \sigma_y \\ \tau_{xy} \end{bmatrix} = \begin{bmatrix} \bar{Q}_{11} & \bar{Q}_{12} & \bar{Q}_{16} \\ \bar{Q}_{12} & \bar{Q}_{22} & \bar{Q}_{26} \\ \bar{Q}_{16} & \bar{Q}_{26} & \bar{Q}_{66} \end{bmatrix}_k \begin{bmatrix} \varepsilon_x^0 \\ \varepsilon_y^0 \\ \gamma_{xy}^0 \end{bmatrix} + z \begin{bmatrix} \bar{Q}_{11} & \bar{Q}_{12} & \bar{Q}_{16} \\ \bar{Q}_{12} & \bar{Q}_{22} & \bar{Q}_{26} \\ \bar{Q}_{16} & \bar{Q}_{26} & \bar{Q}_{66} \end{bmatrix}_k \begin{bmatrix} k_x \\ k_y \\ k_{xy} \end{bmatrix} \tag{5}$$

$$[\sigma] = [\bar{Q}]_k [\varepsilon^0] + z[\bar{Q}]_k [k] \tag{6}$$

and the equations for stress and moment resultants given in vector format (Equations (7) and (8), respectively) in terms of the stress vector, also from Halpin [12] in equations (3-20) and (3-27),

$$
\begin{bmatrix} N_x \\ N_y \\ N_{xy} \end{bmatrix} = \int_{-h/2}^{h/2} \begin{bmatrix} \sigma_x \\ \sigma_y \\ \tau_{xy} \end{bmatrix} dz \tag{7}
$$

$$
\begin{bmatrix} M_x \\ M_y \\ M_{xy} \end{bmatrix} = \int_{h_{k-1}}^{h_k} \begin{bmatrix} \sigma_x \\ \sigma_y \\ \tau_{xy} \end{bmatrix} z\ dz \tag{8}
$$

the ABD matrix can be calculated. The result of combining the Halpin equations is given in detail in Ochoa–Redding [8] as:

$$
\begin{Bmatrix} N_1 \\ N_2 \\ N_6 \end{Bmatrix} = \begin{bmatrix} A_{11} & A_{12} & A_{16} \\ A_{12} & A_{22} & A_{26} \\ A_{16} & A_{26} & A_{66} \end{bmatrix} \begin{Bmatrix} \varepsilon_1^{(0)} \\ \varepsilon_2^{(0)} \\ \varepsilon_6^{(0)} \end{Bmatrix} + \begin{bmatrix} B_{11} & B_{12} & B_{16} \\ B_{12} & B_{22} & B_{26} \\ B_{16} & B_{26} & B_{66} \end{bmatrix} \begin{Bmatrix} \varepsilon_1^{(1)} \\ \varepsilon_2^{(1)} \\ \varepsilon_6^{(1)} \end{Bmatrix} \tag{2.4-23a}
$$

$$
\begin{Bmatrix} M_1 \\ M_2 \\ M_6 \end{Bmatrix} = \begin{bmatrix} B_{11} & B_{12} & B_{16} \\ B_{12} & B_{22} & B_{26} \\ B_{16} & B_{26} & B_{66} \end{bmatrix} \begin{Bmatrix} \varepsilon_1^{(0)} \\ \varepsilon_2^{(0)} \\ \varepsilon_6^{(0)} \end{Bmatrix} + \begin{bmatrix} D_{11} & D_{12} & D_{16} \\ D_{12} & D_{22} & D_{26} \\ D_{16} & D_{26} & D_{66} \end{bmatrix} \begin{Bmatrix} \varepsilon_1^{(1)} \\ \varepsilon_2^{(1)} \\ \varepsilon_6^{(1)} \end{Bmatrix} \tag{2.4-23b}
$$

where A_{ij} denote the extensional stiffnesses, D_{ij} the bending stiffnesses, and B_{ij} the bending-extensional stiffnesses of a laminate:

$$
(A_{ij}, B_{ij}, D_{ij}) = \sum_{k=1}^{N} \int_{z_k}^{z_{k+1}} Q_{ij}^{(k)} (1, z, z^2) dz \tag{2.4 -24a}
$$

where $Q_{ij}^{(k)}$ are the material stiffnesses of the k-th lamina, as referred to the laminate coordinates [8].

The examples given by the two texts vary in the level of detail given to the derivation, but they reach the same conclusion and which is written most simply in Equation (9) from Halpin [12] as the total plate constitutive equation:

$$
\begin{bmatrix} N \\ \cdots \\ M \end{bmatrix} = \begin{bmatrix} A & \vdots & B \\ \cdots & \cdots & \cdots \\ B & \vdots & D \end{bmatrix} \begin{bmatrix} \varepsilon^0 \\ \cdots \\ k \end{bmatrix}
\tag{9}
$$

2.   Using the ABD–Matrix

The usefulness of the ABD matrix for this thesis is with the application to the orthotropic laminate of the nose fairing in the calculations within the ANSYS program. When a laminate is orthotropic and symmetric it has properties that further simplify the "extensional stiffness" ([A] matrix), "bending–extensional stiffness" ([B] matrix) and "bending stiffness" ([D] matrix) matrices within the ABD Matrix.

For a laminate that has mid–plane symmetry Halpin shows, using Equation (10), that lamina opposite each other with the same properties and orientations cause the values for each B_{ij} to be zero. This means that there is no bending membrane coupling for this configuration [12].

$$
Bij = \frac{1}{2} \sum_{k=1}^{n} \left(\bar{Q}_{ij} \right)_k \left(h_k^2 - h_{k-1}^2 \right)
\tag{10}
$$

It is further shown that the [A] and [D] matrices are similarly simplified by constructing a symmetric laminate with opposing lamina in a cross ply pattern with the lamina angles opposing, such as a 5 layer laminate with plys oriented from top to bottom 90/–90/0/–90/90 [12]. The result for the [A] matrix is the values for A_{16} and A_{26} in Equation (2.4 23a from [8]) to be zero and the matrix to be specially orthotropic. While the [D] matrix does not reduce as quickly as [A], it is shown that by using more plys, the values for D_{16} and D_{26} Equation (2.4 23b from [8]) are heading to a zero limit. This indicates that an increase in the number of plys also drives the [D] matrix closer to being specially orthotropic [12].

The significance of the simplification of the ABD matrix as described is that the [A] matrix and [D] matrix can be used in calculations for analyzing the laminate numerically via the laminate plate theory. With the material properties, lamina thickness, ply orientation and the number of lamina an ABD matrix describing the properties of a

laminate can be calculated. The properties now defined by the extensional stiffness matrix [A] and bending stiffness matrix [D] can be entered directly into ANSYS under the "Linear Elastic" tab in a table for "Anisotropic Elasticity."

C.   MATERIAL PROPERTIES

1.   Sitka Spruce

The description of Sitka spruce in the Wood Handbook [13] does not make it sound like the structural workhorse required for the D5 nose fairing requires.

> The wood has a comparatively fine, uniform texture, generally straight grain, and no distinct taste or odor. It is moderately lightweight, moderately low in bending and compressive strength, moderately stiff, moderately soft, and moderately low in resistance to shock. It has moderately low shrinkage. On the basis of weight, Sitka spruce rates high in strength properties and can be obtained in long, clear, straight–grained pieces [13].

But, due to its favorable physical characteristics of high strength for low weight, and being easy to work, Sitka spruce has long been the most important wood used for aviation construction [13]. The prevalence of Sitka spruce in early aviation is evidenced in the popular misnomer given to Howard Hughes' H–4 Hercules, the Spruce Goose. Though the plane was made of wood, it was mostly birch, not the spruce that was implied [14]. The continuing prominence of this wood species as a dominant aviation construction material can be appreciated by reading the study from 2009 by Cairns and Wood aimed at identifying potential replacement materials [15], in which Sitka spruce is described as "the standard against which all other woods are judged."

a.   Orthotropic Nature of Wood

Like most woods, Sitka spruce is an orthotropic material, having independent mechanical properties in three perpendicular planes with respect to the growth rings of the tree as in Figure 4. The axes of the planar directions are described as Longitudinal (L), Radial (R), and Tangential (T). As discussed in the Wood Handbook [13] to describe the elastic properties of wood nine of twelve constants must be known,

consistent with previous discussion of orthotropic composites. These constants are the moduli of elasticity (*E*), moduli of rigidity (*G*), and Poisson's ratios (µ) of the wood in the x, y, and z directions.
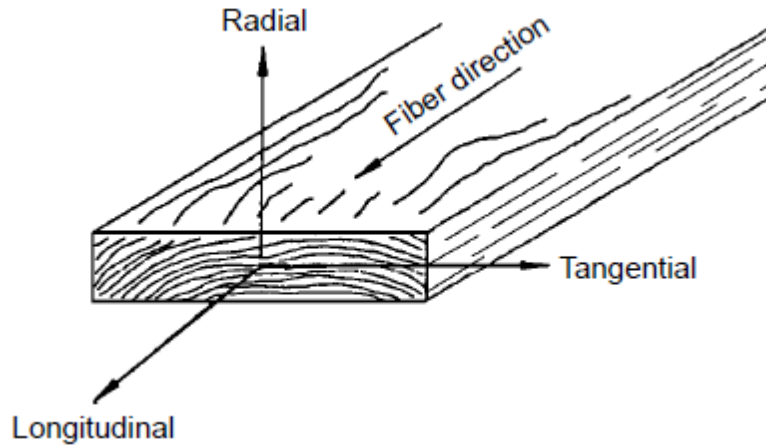
Figure 4.   Three Principle Axes of Wood with Respect to Grain Direction and Growth Rings (From [13])

b.   *Selection*

Sitka spruce to be used in air and space applications is expected to have predictable material characteristics. To ensure this is true, the selection of wood used in these applications must be of the highest quality. Only wood that has clear straight grain with minimal knotting and pitch pockets is selected to prevent failure of the structures in the stressful environments of air and space flight.

2.   Fiberglass and Resin

Fiberglass is the name used for a composite of glass fibers woven into a cloth fabric imbedded in a resin. A benefit of the cloth construct of the glass fibers is the ability for fiberglass to be molded into a variety of complex shapes prior to the solidification of the form achieved when the resin component has hardened or "set." The resin also acts as a bonding agent when the fiberglass is built into a laminate, as found in the nose fairing.

16

There are a variety of types of cloth and resin used for different applications. Using an older military specification [16] for fiberglass as a guide, it is assumed for this thesis that the cloth is Type II which is indicated to support the use of epoxy resin. This cloth is described by tables in the military specification as being of plain weave, thickness between 0.0035 and 0.0055 inches, and having a minimum average tensile strength of 47 kpsi.

D.   TESTING

To provide a proper foundation for validating the computer model, standardized testing methods were identified. Nominal test modes based on the expected loading of the nose fairing were determined to be tension and compression. Two Department of Defense approved American Society for Testing and Materials (ASTM) International standards were chosen for potential application to the process; Standard Test Methods for Structural Panels in Tension (ASTM D3500) [17] and Standard Test Methods for Wood-Based Structural Panels in Compression (ASTM D3501) [18]. While both tests should be conducted in the comprehensive evaluation of the nose fairing and any material choices, only the tension test is used for this thesis.

1.   Test Method Selection

ASTM D3500 provides two test methods for evaluating the tensile properties of structural panels. Test Method A is for small specimens and Test Method B is for large specimens [17]. Method A was determined to be the best choice for the purpose of this thesis for two reasons. First, to facilitate testing it is desirable to use a smaller sample size to limit the expense of sample materials and large testing equipment. Second, ASTM D3500 Standard describes Method A as being "suited to material that is uniform with respect to tensile properties." This describes the material quality and processing that is expected to be used on the nose fairing. Method B is described by ASTM D3500 as "respond(ing) well to all manufacturing variables and growth characteristics that affect the tensile properties of structural panels." This could make Method B a good choice for

17

evaluating how reduced standards of material and process control would affect the nose fairing. Evaluation using this method may prove useful in future Sitka spruce laminate tests as premium quality material becomes scarcer.

2. Specimen Type Selection

For Method A, there are three specimen types that can be used, as seen in Figure 5. The three types are A, B, or C; with the differences in the specimens being mostly in the gage width and length, and specimen width. In a test specimen, the gage is the section of the material that is to be measured during the test. This section is specially dimensioned to reduce the amount of measured distortion due to the test set up and apparatus attachment to the specimen. Specimen Type A was chosen based on the guidance for its use with laminates having grain angles of 0° or 90° and material over a quarter inch in thickness, both of which correspond to the nose fairing laminate.

U.S. Customary Units, in.	Metric Equivalents mm	U.S. Customary Units, in.	Metric Equivalents mm
¼	6	3⅞	98
½	13	4⅛	105
1	25	4¼	108
1⅞	48	16	406
2½	64	20	503
2⅝	67	25	635
2⅞	73	30	762

Figure 5.   Dimensions and Details of Tension Test Specimens (From [17])

THIS PAGE INTENTIONALLY LEFT BLANK

III. MODELING AND ANALYSIS

A. ANSYS

The software used for the modeling and analysis for this thesis is ANSYS 13.0. ANSYS is a suite of suite of simulation analysis tools that can be used to evaluate computer generated models for a variety of engineering applications. Information such as material data, geometry constraints, and environment are used to define the model fully for the software. With a well–defined model, ANSYS analysis tools can be used to perform computational evaluation to provide solution output data about the model, such as stress, strain, and material deformation.

B. COUPON MODELS

Without comparing output information from software evaluations with real data, it would be imprudent to assume that a computer model and simulation accurately represents the physical structure and properties. A standard basis to evaluate the software analysis is necessary. To facilitate validation of the ANSYS output data, the three models were developed as phases of the composite analysis. The dimensions are based on the ASTM D3500 Standard Test Method A, Specimen Type A.

Lamina thicknesses for these samples were chosen based on an assumed nose fairing thickness of approximately 0.5 inches. The number of each Sitka and fiberglass lamina was also a factor used in determining the nominal thickness used. The fiberglass thickness of 0.005 inches was based on the descriptions for government approved fiberglass materials in the Milstandard [16]. Sitka lamina thickness of 0.05 inches is consistent with standard veneer thicknesses and gives a total thickness of 0.45 inches of wood in the laminate. A final laminate thickness of 0.49 inches was achieved with these assumptions and is accepted as sufficiently close to assumed nose fairing thickness.

For analysis of the models, material properties must be chosen in ANSYS under the Engineering Data heading and assigned to each "part." The library of materials in ANSYS did not provide information for Sitka spruce or fiberglass and new materials were defined to support modeling the nose fairing laminate. Table 2 shows the data

entered in the Engineering Data library for both. An online material properties data reference, www.MATWEB.com, was used to define the properties. Comparing the information to various other references, the properties listed for "American Sitka spruce wood" and "E–glass fiber, generic" were chosen as the representative characteristics. The MATWEB data sheets are included as Appendices A and B [21 and 22].

Sitka Spruce as entered into ANSYS			E-Fiberglass as entered into ANSYS		
Property	Value	Unit	Property	Value	Unit
Density	0.013	lb in^-3	Density	0.092	lb in^-3
Orthotropic Elasticity			Isotropic Elasticity		
Young's Modulus X direction	1600000	psi	Derived from -->	Young's Modulus and	
Young's Modulus Y direction	130000	psi	Young's Modulus	10500000	psi
Young's Modulus Z direction	69000	psi	Poisson's Ratio	0.2	
Poisson's Ratio XY	0.37		Bulk Modulus	40219433333	Pa
Poisson's Ratio YZ	0.44		Shear Modulus	30164575000	Pa
Poisson's Ratio XZ	0.47		Tensile Ultimate Strength	75500	psi
Shear Modulus XY	102000	psi			
Shear Modulus YZ	48000	psi			
Shear Modulus XZ	98000	psi			
Tensile Ultimate Strength	230	psi			

Table 2.   ANSYS Sitka Spruce and Fiberglass Engineering Data (After [21], [22])

1.   Initial Model—Coupon A: 0º Sitka Sample

The first coupon sample to be built, Coupon A is of the simplest design. Dimensions from Tension Test Specimen A, of Method A described in section II.d.2 and shown in Figure 5, are used as a basis for modeling. First a length and width sketch was drawn. On this sketch, the gage section and the transition curve are outlined. The transition and gage section sketch was combined with the first sketch to form the base sketch from which the lamina are built.

Lamina layers were extruded from the base sketch for each of the two different lamina thicknesses. Copies of the lamina layers were made and positioned to make each face adjacent with the representative fiberglass and wood layers alternating. The adjoining faces were then defined to be bonded together for the purpose of analysis. Figure 6 shows the base sketch with lamina extrusions.
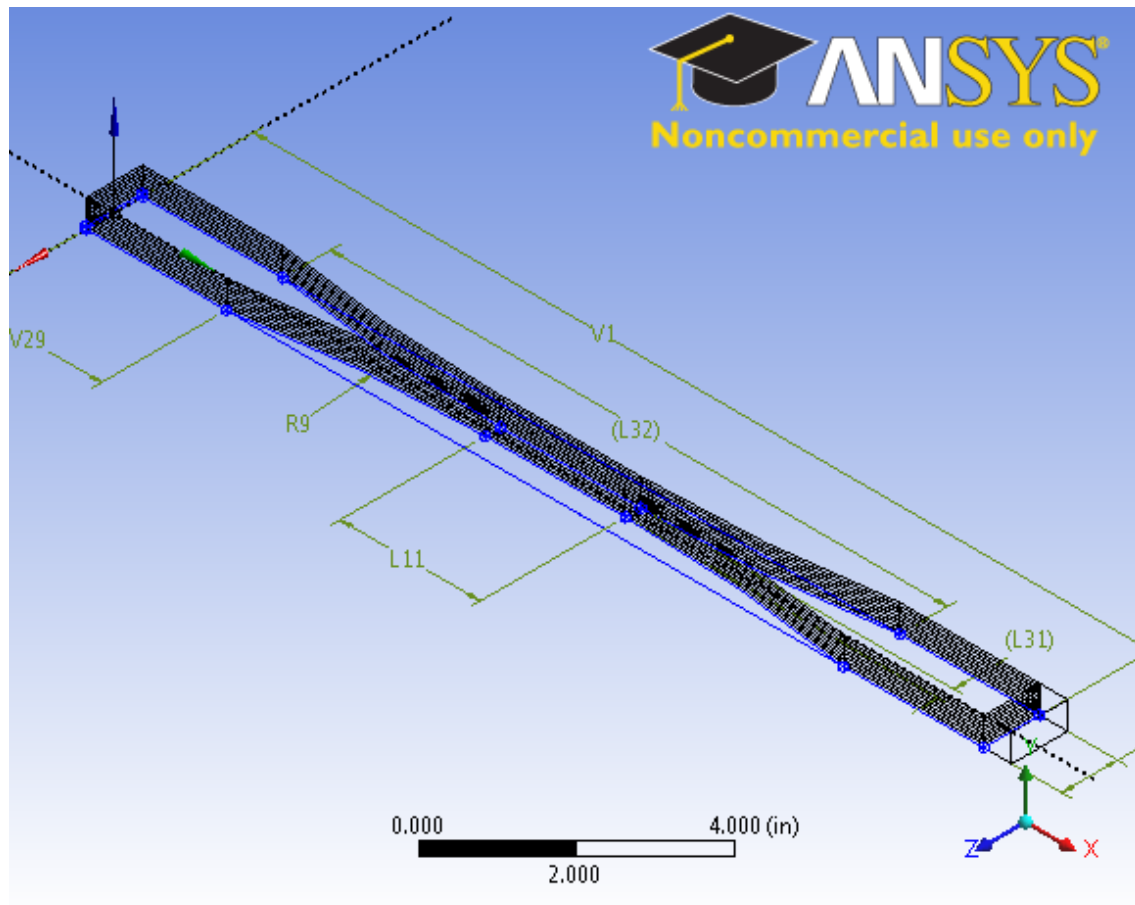
Figure 6.   Basic ANSYS Coupon Sketch with Lamina Extrusions

During an initial attempt to apply a force, it was shown that the force would not be applied evenly across the lamina when attached to the end of a single lamina in the stack. To artificially alleviate this anomaly, an attachment point was built into the model. This attachment point is a part of the same dimension as the end of a coupon. The part is bonded to the ends of all lamina at the point of application of the force. With the idea of minimizing distortion of the analysis results, the attachment part was defined to be made of steel. Properties for structural steel found in the ANSYS Engineering Data library are used for this part as shown in Table 3.

Structural Steel from ANSYS Engineering Data Library					
Property	Value	Unit	Property	Value	Unit
Density	7850	kg m^-3	Strain-Life Parameters		
Isotropic Secant Coefficient of Thermal Expansion			Display Curve Type	Strain-Life	
Coefficient of Thermal Expansion	1.20E-05	C^-1	Strength Coefficient	920000000	Pa
Reference Temperature	22	C	Strength Exponent	-0.106	
Isotropic Elasticity			Ductility Coefficient	0.213	
Derived from -->	Young's Modulus and Poisson's Ratio		Ductility Exponent	-0.47	
			Cyclic Strength Coefficient	1000000000	Pa
Young's Modulus	2E+11	Pa	Cyclic Strain Hardening Exponent	0.2	
Poisson's Ratio	0.3		Tensile Yield Strength	250000000	Pa
Bulk Modulus	1.66667E+11	Pa	Compressive Yield Strength	250000000	Pa
Shear Modulus	76923076923	Pa	Tensile Ultimate Strength	460000000	Pa
Alternating Stress Mean Stress	Tabular		Compressive Ultimate Strength	0	Pa
Interpolation	Log-Log				
Scale	1				
Offset	0	Pa			

Table 3.   Structural Steel Engineering Data

2.   Coupon B: 0º and 90º Sitka Sample

A second coupon sample was built in ANSYS to continue the iteration toward the final composite coupon. This coupon uses the initial model as a base with a change in the lamina orientation. Every other Sitka spruce lamina was alternated by an angle of 90° from the center axis of the coupon.

A complication was identified with the basic premise of orienting the lamina. Due to the orthotropic nature of the wood, it is not correct to simply substitute the x and y material property values for the spruce to define a change in orientation. A transformation equation must be used to reorient the material properties to properly define them with regard to the normal axis of the sample. This discovery was made intuitively and confirmed by the Ochoa–Reddy text [8] in Equation (11). Calculated data used for material properties of the 90° orientation of spruce is shown in Table 4.

$$\begin{Bmatrix} \bar{\sigma}_1 \\ \bar{\sigma}_2 \\ \bar{\sigma}_6 \end{Bmatrix} = \begin{bmatrix} \cos^2\theta & \sin^2\theta & 2cos\theta\sin\theta \\ \sin^2\theta & \cos^2\theta & -2\cos\theta sin\theta \\ -\cos\theta\sin\theta & \cos\theta\sin\theta & \cos^2\theta - \sin^2\theta \end{bmatrix} \begin{Bmatrix} \sigma_1 \\ \sigma_2 \\ \sigma_6 \end{Bmatrix} \qquad (11)$$

90° Oriented Spruce (Sitka 2) as entered in ANSYS		
Property	Value	Unit
Density	0.013	lb in^-3
Orthotropic Elasticity		
Young's Modulus X direction	69000	psi
Young's Modulus Y direction	130000	psi
Young's Modulus Z direction	1600000	psi
Poisson's Ratio XY	0.24	
Poisson's Ratio YZ	0.029	
Poisson's Ratio XZ	0.02	
Shear Modulus XY	48000	psi
Shear Modulus YZ	102000	psi
Shear Modulus XZ	98000	psi
Tensile Ultimate Strength	230	psi

Table 4.   Material Properties of 90° Sitka Spruce Lamina

3.   Coupon C: ABD Matrix Sample

The last model for coupon analysis is the coupon built with material properties defined by the D Matrix. Dimensions of the overall coupon are the same as Coupons A and B. Individual laminae were removed to define the coupon as a single plate. Further validation would be required, but this method of modeling could potentially provide the most representative data.

For expedience, calculation of the ABD matrix for the coupon is made using established programs. Values from an online ABD matrix calculator found on the Efunda website [19] are used after a MATLAB program provided by Professor Ramesh Kolar has verified the computations. Laminae were defined as alternating zero and 90 degree Sitka spruce plys with 45 degree fiberglass plys between each. Table 5 shows the values as entered into ANSYS and the Efunda calculation is in Appendix C [19].

Spruce Fiberglass Laminate from ABDmatrix					
(psi)	(psi)	(psi)	(psi)	(psi)	(psi)
850.1					
109.5	778.7				
0	0	219.1			
0	0	0	1.56E+13		
0	0	0	1.703E+12	1.158E+13	
0	0	0	0.000621	0.006672	3.415E+12

Table 5.   Spruce and Fiberglass Laminate ABD Calculated Properties

C.   NOSE FAIRING MODEL

Dimensions for the nose fairing model are taken from the drawing in Figure 7 and extrapolations made for those shown in Figure 8. The diameter at the base of the nose fairing is shown to be 81'' ({'L3'+'L9'} x2) and overall length is set at the given 80.8'' ('L11'). An estimation of the cylindrical length before the diameter of the nose fairing begins to decrease is not made. Instead, an estimated 108" radius of the curve of the nose fairing ('R6') was established by trial and error that appeared to best represent the figure, yielding a final inside diameter at the nose cone interface of 58.87" ('L4' x2).
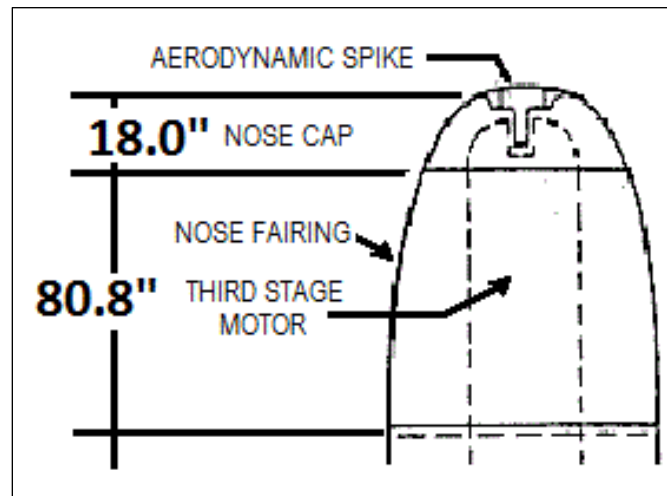

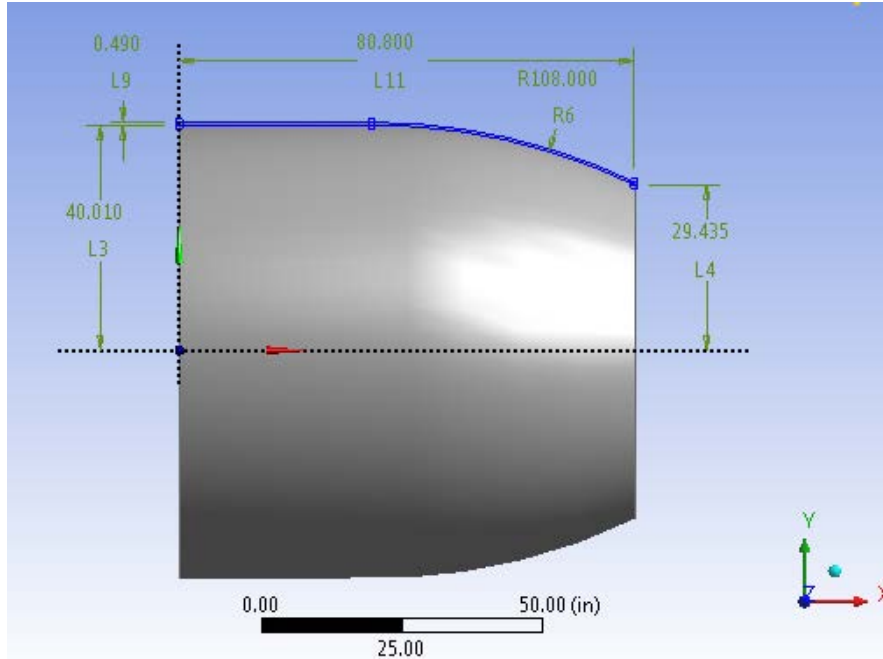Figure 7.   Nose Fairing Height (From [20])

Figure 8.   Nose Fairing Dimensions

A shell was formed by revolving the base sketch of the dimensions. The model of the nose fairing is built as a simplified version of the actual nose fairing. To alleviate difficulties encountered in early analysis attempts, the aluminum rings at the base and tip of the nose fairing are not modeled. Additionally, no fittings for cabling and separation rockets are part of the model. Properties of the model are the same as those entered for Coupon C in Table 5.

D.   ANALYSIS

1.   Coupons

Each of the coupons is analyzed in ANSYS using the same method to simulate a tension test. One end of the coupon is defined to have a fixed support. The other end has a force of 177 lbs applied. This force is established based on the cross sectional area of the coupons being 0.1225 in^2 (0.25 in x 0.49 in), compared to the overall cross sectional area of the nose fairing at the smallest diameter carrying the full 130,000 lbs. during lifting.

Solutions for three elements of the problem are solved to evaluate how the coupon models compare. These elements are equivalent stress, directional deformation, and total deformation. Each of the coupon models show different results due to the change in how the models are constructed.

a.   *Equivalent Stress*

The maximum equivalent stress calculated is for Coupon B at 8,263 psi. Coupon A and C are 6,045 psi and 1,347 psi respectively. A screen shot of the stresses in Coupon B from ANSYS is shown as Figure 9. Zooming into the maximum stress for Coupons A and B in Figures 10 and 11 shows that the stress is located in a middle ply for Coupon A and outer ply for Coupon B. This difference in location of maximum stress could be a result of how the properties of the lamina are defined. In an actual coupon sample being tested the point of maximum stress could be the start of a delamination or the initiation of laminate failure.
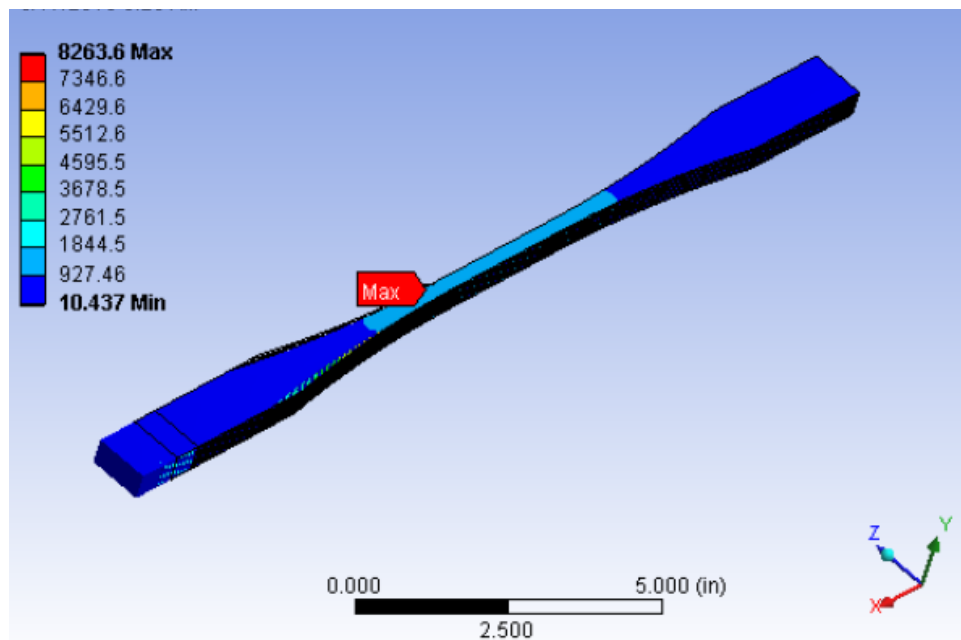

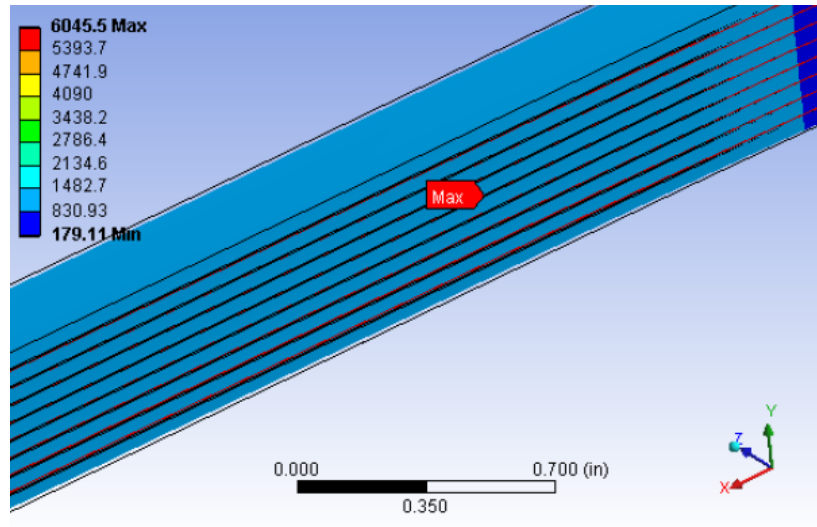Figure 9.   Coupon B Maximum Stress Screen Shot

Figure 10.   Coupon A Max Stress in Mid–Ply Fiberglass Lamina
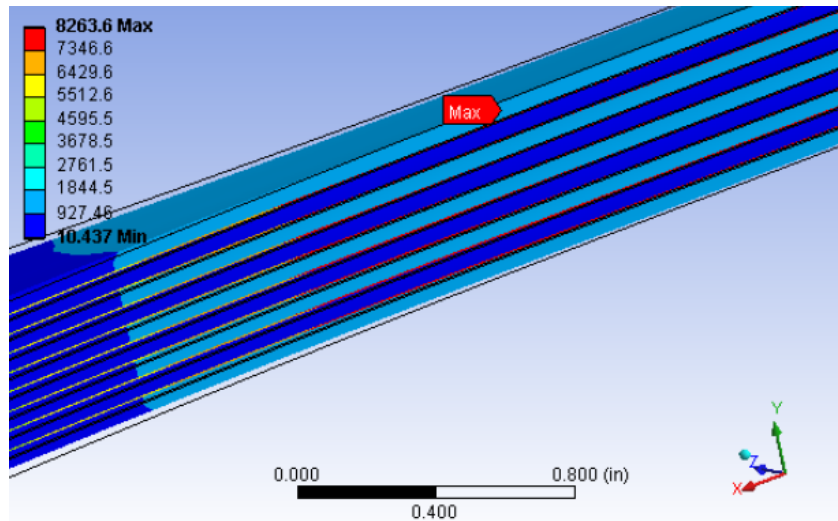

Figure 11.   Coupon B Max Stress in Outer–Ply Fiberglass Lamina

The results for Coupon C show a much-reduced maximum stress. Due to the nature of the material properties being defined to represent Coupon C as a single plate, there are no interactions between plys and any localized stress is neglected. Figure 12 shows Coupon C.
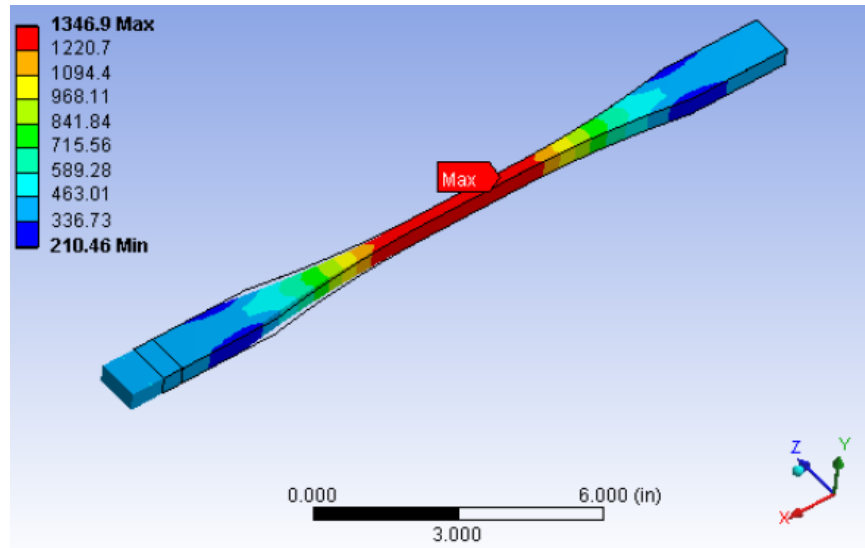
Figure 12.   Coupon C Equivalent Stress

b.   Deformation

Deformation of the coupons is reported in directional and total values for comparison between samples. Results show that the deformation in the direction of the axis of tension is the only direction of significance for the coupons.   All coupons deformed lengthwise less than 10 thousandths of an inch in the analysis, with the smallest deformation in Coupon A (shown in Figure 13).

Figure 13.   Coupon A Total Deformation Screen Shot

2. Nose Fairing

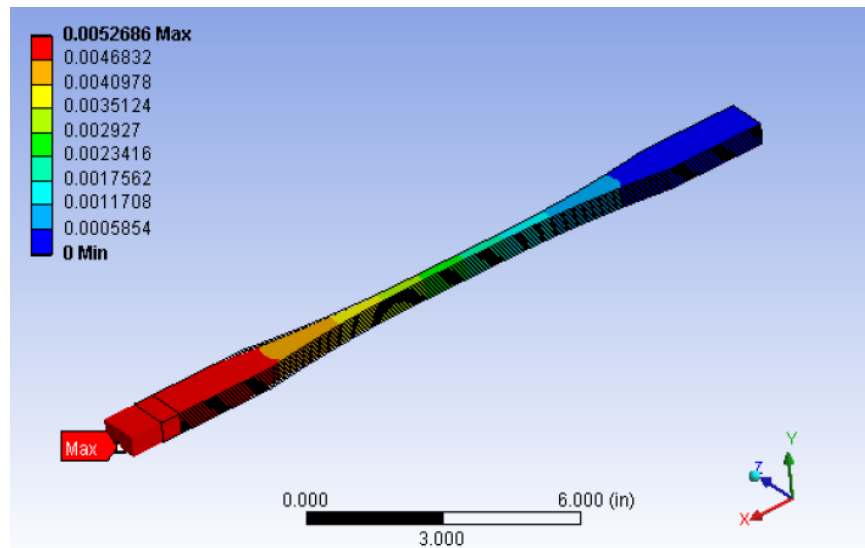Similar to the coupon models, the nose fairing is analyzed in tension. A force is applied at the leading face on the tip of the nose fairing, while the base is defined as a fixed support. The force is defined to be 130,000 lbs. to represent the full weight of the missile as if it is being lifted. The analysis is reported with the same three elements as the coupons. Color coded screen shots from ANSYS show the tip of the nose fairing is where most of the stress and deformation are found with a maximum equivalent stress of 14,219 psi and deformation of 0.05 in. Screen shots for each of the results are shown in Figures 14, 15, and 16.
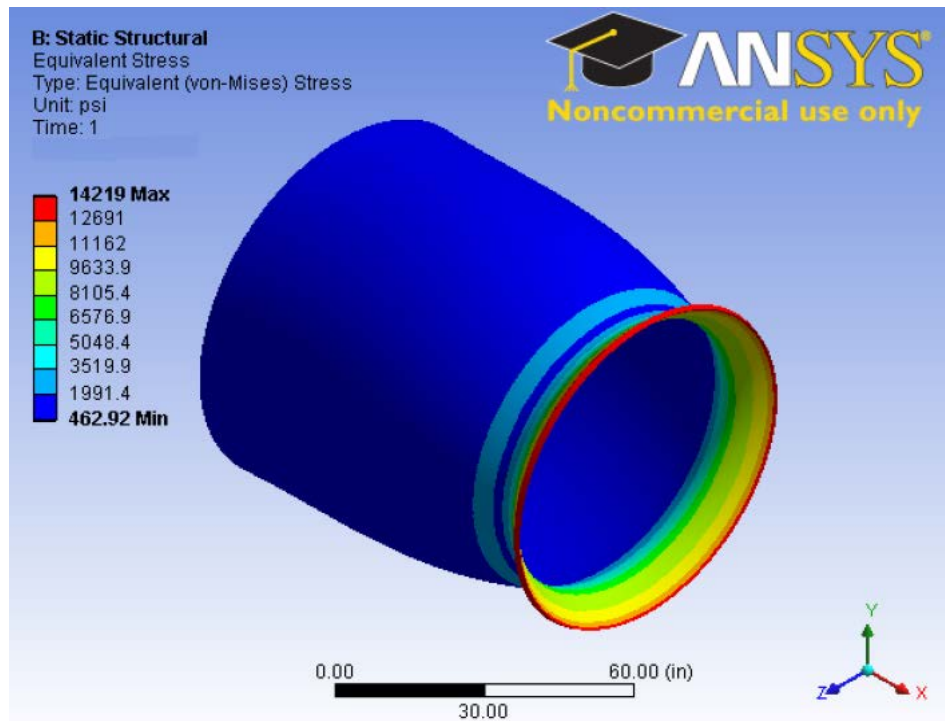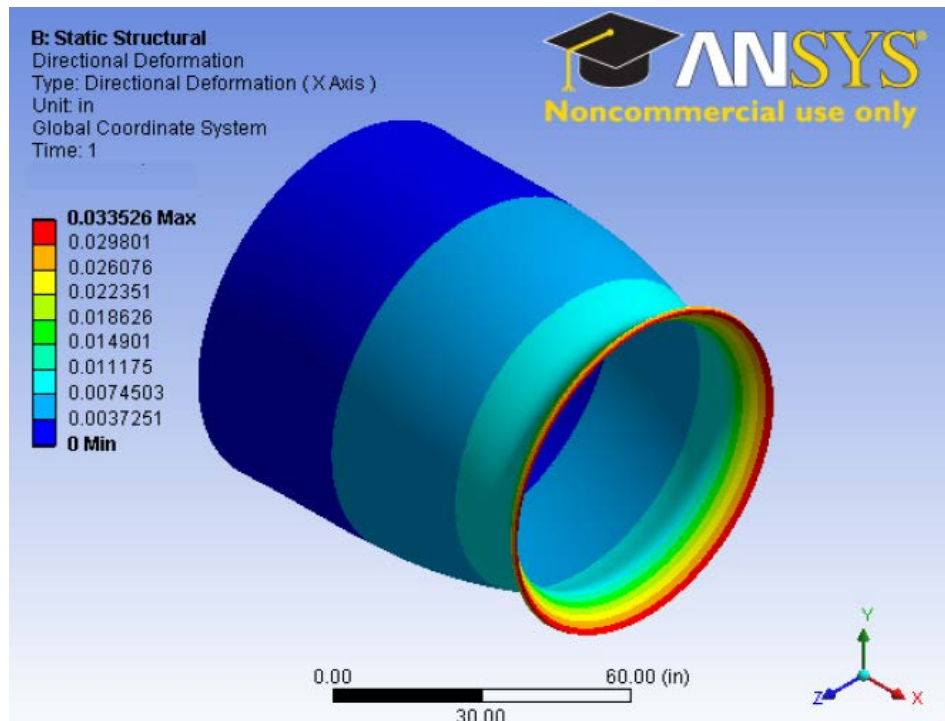

Figure 14.   Nose Fairing Equivalent Stress
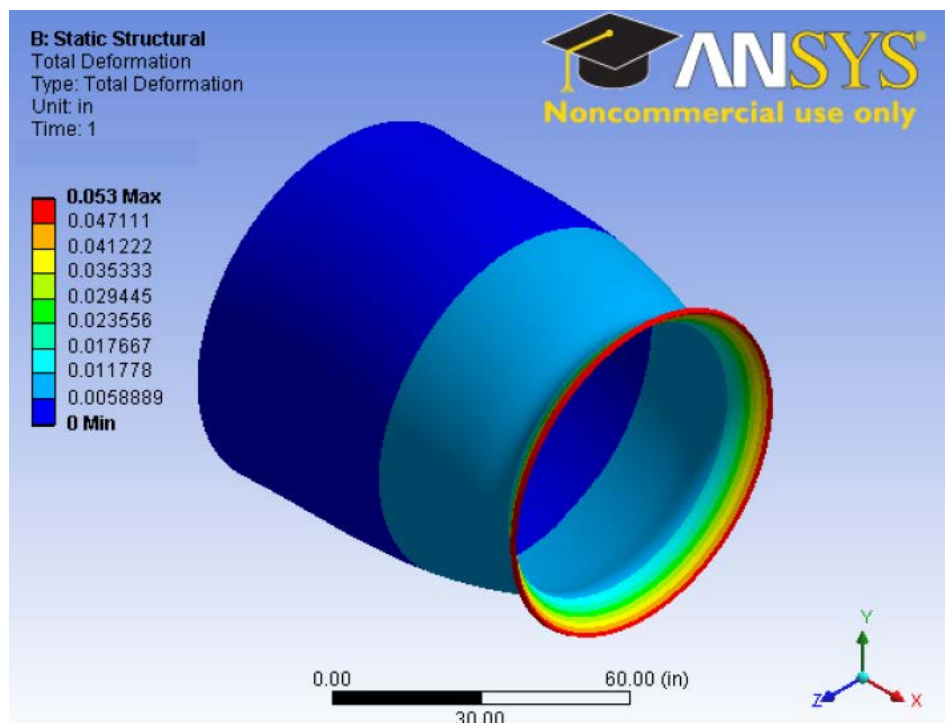
Figure 15.　　　Nose Fairing Directional Deformation

Figure 16.　　　Nose Fairing Total Deformation

IV. CONCLUSION AND RECOMMENDATIONS

A. CONCLUSION

A computer model generated to represent a real complex object is not difficult to build. Putting into the model the right dynamic properties in a way that will allow for realistic calculations is more challenging. ANSYS shows really promising results with the models built of the coupons and nose fairing. For use in real world analysis of the system more work should be done to verify the program is calculating valid results.

This work proved to be a successful first attempt to develop a method to evaluate the ANSYS program as a tool for analysis of the D5 missile nose fairing. Testing methods for model validation were identified. Coupons of differing levels of complexity were modeled and analyzed with the software. Finally, a representative model of the nose fairing was built and analyzed.

Further effort spent refining the models and conducting validation testing should establish the full benefit of using a model and simulation tool such as ANSYS as an efficient and cost saving method to analyze the nose fairing in the future.

B. RECOMMENDATIONS

1. Verification, Validation, and Accreditation

This thesis could be the first step in using a computer to save time and money evaluating a proven design. Before any modeling and simulation software can be used in a government acquisition it must be tested to prove that it will work properly, produce valid results, and satisfactorily accomplishes the task for which it will be used. This process is known as verification, validation, and accreditation (VV&A).

While the data presented is promising, additional testing should be conducted to validate the computer modeling of the laminate and nose fairing. As discussed previously, testing with physical samples is initially costly, but provides a basis for more extensive use of computer models in the future. Properly validated, the digital tools can

be used to predict how changes in the material and dimensional properties will be effected before building and testing is conducted on "real" samples.

It is seen that this method of design appraisal could facilitate taking leaps to newer materials that might not be affordable if physical testing was the only means to evaluate the change. This gives rise to new opportunities for assessing the design trade space of the nose fairing. With the various analyses available (and being added all the time) it may open up new avenues to determine the relative "health" of the nose fairings already in the field or those that may be constructed to supplement the supply.

2. Further Testing

a. *Better Software?*

The choice of software used in this thesis was made based on the intended application, but it was influenced on availability as well. In the course of developing this thesis, an additional analysis tool unavailable for use under the NPS license was identified that may prove to be more useful in the nose fairing analysis. AUTODYN Composite Modeling is available from ANSYS that is designed specifically for the unique attributes of composites. There are also many other modeling and simulation programs available and others are surely being developed.

b. *Model Validation*

Coupon and full nose fairing tests should be conducted. These are necessary for the VV&A process, but could provide further insight into what to model or analyze for. Determining the failure mechanism of a composite can provide a way forward to a better composite design for the application. Tests can be designed based on the software analysis that may provide non–destructive methods to evaluate integrity of nose fairings as well.

APPENDIX A.   MATWEB AMERICAN SITKA SPRUCE WOOD

American Sitka Spruce Wood

Categories:	Wood and Natural Products; Wood; Softwood

Material Notes: Softwood. Relatively easy to work with hand tools. Data is based on small, clear, air-dried samples unless specified.
Usual surface texture: Coarse
Dimensional changes when dried lumber is subjected to variations in humidity during service: Small
Resistance to fungal decay (Heartwood in ground contact): Non-durable (5 to 10 years)
Resistance to penetration by preservatives: Resistant
Common Applications: Construction, packaging, pallets

Property values marked by an asterisk (*) have been taken from an unusually old reference source.

Key Words: *Picea sitchensis*; Lumber, Timber
Vendors: No vendors are listed for this material. Please click here if you are a supplier and would like information on how to add your listing to this material.

Physical Properties	Metric	English	Comments
Density	0.310 - 0.360 g/cc	0.0112 - 0.0130 lb/in³	Earlywood
	0.370 g/cc	0.0134 lb/in³	Oven Dry Weight/Unseasoned Volume
	0.529 g/cc	0.0191 lb/in³	Unseasoned*
	0.550 - 0.870 g/cc	0.0199 - 0.0314 lb/in³	Latewood
Water Absorption	0.500 - 3.50 %	0.500 - 3.50 %	Between 40% RH and 90% RH

Mechanical Properties	Metric	English	Comments
Hardness, Wood Indentation	1600 N	360 lb (f)	Side. Force required to imbed a 0.444 inch steel ball to one-half its diameter*
	1900 N	427 lb (f)	End. Force required to imbed a 0.444 inch steel ball to one-half its diameter*
Tensile Strength, Ultimate	1.59 MPa	230 psi	Perpendicular to Grain*
Modulus of Rupture	0.0379 GPa	5.50 ksi	Static Bending*
	0.0700 GPa	10.2 ksi	In Bending
Flexural Modulus	8.14 GPa	1180 ksi	Static Bending*
	11.0 GPa	1600 ksi	In Bending
Flexural Yield Strength	20.7 MPa	3000 psi	Fiber Stress at Elastic Limit; Static Bending*
	46.2 MPa	6700 psi	Bending stress at proportional limit
Compressive Yield Strength	2.28 MPa	330 psi	Perpendicular to Grain*
	15.7 MPa	2280 psi	Parallel to Grain*
	17.9 MPa	2600 psi	Max Crushing Strength Parallel to Grain*
	38.6 MPa	5600 psi	Parallel to Grain
Poissons Ratio	0.0250	0.0250	μ_{TL}, 12% Moisture Content
	0.0400	0.0400	μ_{RL}, 12% Moisture Content
	0.245	0.245	μ_{TR}, 12% Moisture Content
	0.372	0.372	μ_{LR}, 12% Moisture Content
	0.435	0.435	μ_{RT}, 12% Moisture Content
	0.467	0.467	μ_{LT}, 12% Moisture Content
Machinability	100 %	100 %	Good Relative to Other Wood
Shear Strength	5.38 MPa	780 psi	Parallel to Grain*
Impact	2.50	2.50	in-lb/in³; Work to Elastic Limit; Unseasoned Sample; Impact Bending*
	7900	7900	psi; Fiber Stress at Elastic Limit; Unseasoned Sample; Impact Bending*
Work to Elastic Limit	0.00303 J/cm³	0.440 in-lb/in³	Static Bending*
Work to Maximum Load	0.0441 J/cm³	6.40 in-lb/in³	Static Bending*

Thermal Properties	Metric	English	Comments
CTE, linear	5.40 µm/m-°C @Temperature 20.0 °C	3.00 µin/in-°F @Temperature 68.0 °F	Axial. Typical value for Spruce.
	6.30 µm/m-°C @Temperature 20.0 °C	3.50 µin/in-°F @Temperature 68.0 °F	Radial; Typical value for Spruce.
	34.1 µm/m-°C @Temperature 20.0 °C	18.9 µin/in-°F @Temperature 68.0 °F	Tangential. Typical value for Spruce.
Shrinkage	4.30 %	4.30 %	Radial; Unseasoned to Oven Dry*
	7.50 %	7.50 %	Tangential; Unseasoned to Oven Dry*

Descriptive Properties			
Color		Pinkish-brown	Usual for heartwood

THIS PAGE INTENTIONALLY LEFT BLANK

APPENDIX B.   MATWEB E–GLASS FIBER, GENERIC

E-Glass Fiber, Generic

Categories:	Ceramic; Glass; Glass Fiber; Other Engineering Material; Composite Fibers
Material Notes:	Used as a reinforcing agent in fiber glass composites, including biomedical/surgical applications.
	Information provide by Owens Corning and the reference(s).
Vendors:	No vendors are listed for this material. Please click here if you are a supplier and would like information on how to add your listing to this material.

Physical Properties	Metric	English	Comments
Density	2.54 - 2.60 g/cc	0.0918 - 0.0939 lb/in³	

Mechanical Properties	Metric	English	Comments
Tensile Strength, Ultimate 📊	521 MPa @Temperature -190 °C	75500 psi @Temperature -310 °F	
	1725 MPa @Temperature 540 °C	250200 psi @Temperature 1000 °F	
	2620 MPa @Temperature 370 °C	380000 psi @Temperature 698 °F	
	3450 - 3790 MPa @Temperature 22.0 °C	500000 - 550000 psi @Temperature 71.6 °F	Virgin strength
Elongation at Break	4.80 %	4.80 %	
Modulus of Elasticity	72.4 GPa	10500 ksi	
📊	72.3 GPa @Temperature 540 °C	10500 ksi @Temperature 1000 °F	
Poissons Ratio	0.200	0.200	
Shear Modulus	30.0 GPa	4350 ksi	Calculated

Electrical Properties	Metric	English	Comments
Electrical Resistivity	4.02e+12 ohm-cm	4.02e+12 ohm-cm	
Dielectric Constant 📊	5.90 - 6.40 @Frequency 60 Hz	5.90 - 6.40 @Frequency 60 Hz	
	6.30 - 6.60 @Frequency 1e+6 Hz	6.30 - 6.60 @Frequency 1e+6 Hz	
Dielectric Strength	10.3 kV/mm	262 kV/in	
Dissipation Factor 📊	0.00250 @Frequency 1e+6 Hz	0.00250 @Frequency 1e+6 Hz	
	0.00340 @Frequency 60 Hz	0.00340 @Frequency 60 Hz	

Thermal Properties	Metric	English	Comments
CTE, linear 📊	5.00 µm/m-°C @Temperature 20.0 °C	2.78 µin/in-°F @Temperature 68.0 °F	
	5.40 µm/m-°C @Temperature -30.0 - 250 °C	3.00 µin/in-°F @Temperature -22.0 - 482 °F	
Specific Heat Capacity 📊	0.810 J/g-°C @Temperature 23.0 °C	0.194 BTU/lb-°F @Temperature 73.4 °F	
	1.03 J/g-°C @Temperature 200 °C	0.246 BTU/lb-°F @Temperature 392 °F	
Thermal Conductivity	1.30 W/m-K	9.02 BTU-in/hr-ft²-°F	
Melting Point	<= 1725 °C	<= 3137 °F	
Softening Point	840.6 °C	1545 °F	

Optical Properties	Metric	English	Comments
Refractive Index	1.558	1.558	
	1.562	1.562	bulk annealed

Component Elements Properties	Metric	English	Comments
Al2O3	15.2 %	15.2 %	
BaO	8.0 %	8.0 %	
CaO	17.2 %	17.2 %	
MgO	4.70 %	4.70 %	
NaO2	0.60 %	0.60 %	
SiO2	54.3 %	54.3 %	

Descriptive Properties			
Velocity of sound, m/s		5330	

References for this datasheet.

THIS PAGE INTENTIONALLY LEFT BLANK

APPENDIX C.   EFUNDA ABD CALCULATIONS

Layout of Laminate: [0°/45°/90°/45°/0°/45°/90°/45°/0°/45°/90°/45°/0°/45°/90°/45°/0°]

Number of Lamina Types: There are **2** types of laminae used to construct the laminate.

No.	Lamina Material	E_1	E_2	G_{12}	ν_{12}	$\hbar$
			(Msi)			(mil)
1. Sitka Spruce		1.600	0.1300	0.1020	0.370	48.00
2. Fiberglass		10.50	10.50	4.350	0.200	5.000

Layer Angle   **Lamina Material**

1.	0° 1. Sitka Spruce
2.	45° 2. Fiberglass
3.	90° 1. Sitka Spruce
4.	45° 2. Fiberglass
5.	0° 1. Sitka Spruce
6.	45° 2. Fiberglass
7.	90° 1. Sitka Spruce
8.	45° 2. Fiberglass
9.	0° 1. Sitka Spruce
10.	45° 2. Fiberglass
11.	90° 1. Sitka Spruce
12.	45° 2. Fiberglass
13.	0° 1. Sitka Spruce
14.	45° 2. Fiberglass
15.	90° 1. Sitka Spruce
16.	45° 2. Fiberglass
17.	0° 1. Sitka Spruce

[Previous]   [Start Over]

Results

With the given material properties, the principal stiffness matrices are directly calculated. For directions other than the principal directions, we use the technique discussed in coordinate transformation to calculate the stiffness matrices.

Once we have the stiffness matrix calculated for each layer, the strain-resulatant relations, as seen in the Classical Lamination Theory, are given by

$$
\begin{Bmatrix} N_x \\ N_y \\ N_{xy} \end{Bmatrix} = \begin{bmatrix} A_{11} & A_{12} & A_{16} \\ & A_{22} & A_{26} \\ sym. & & A_{66} \end{bmatrix} \begin{Bmatrix} \varepsilon_x^0 \\ \varepsilon_y^0 \\ \gamma_{xy}^0 \end{Bmatrix} + \begin{bmatrix} B_{11} & B_{12} & B_{16} \\ & B_{22} & B_{26} \\ sym. & & B_{66} \end{bmatrix} \begin{Bmatrix} \kappa_x \\ \kappa_y \\ 2\kappa_{xy} \end{Bmatrix}
$$

$$
\begin{Bmatrix} M_x \\ M_y \\ M_{xy} \end{Bmatrix} = \begin{bmatrix} B_{11} & B_{12} & B_{16} \\ & B_{22} & B_{26} \\ sym. & & B_{66} \end{bmatrix} \begin{Bmatrix} \varepsilon_x^0 \\ \varepsilon_y^0 \\ \gamma_{xy}^0 \end{Bmatrix} + \begin{bmatrix} D_{11} & D_{12} & D_{16} \\ & D_{22} & D_{26} \\ sym. & & D_{66} \end{bmatrix} \begin{Bmatrix} \kappa_x \\ \kappa_y \\ 2\kappa_{xy} \end{Bmatrix}
$$

The results of the extensional stiffness [**A**], the strain-curvature coupling stiffness [**B**], and the bending stiffness [**D**] of the laminate are as follows. Note that the layout begins from top of the laminate as illustrated in the following figure.
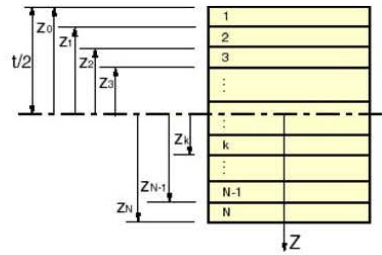
The **extensional stiffness** matrix $[A]$:

$$[A] = \sum_{k=1}^{N} \left(\overline{C}_{ij}\right)_k \left(z_k - z_{k-1}\right) = \sum_{k=1}^{N} \left(\overline{C}_{ij}\right)_k t_k$$

$$= \begin{matrix} 850.1 & 109.5 & 0 \\ 109.5 & 778.7 & 0 \\ 0 & 0 & 219.1 \end{matrix} \quad \text{Msi-mil}$$

where $[\overline{C}]_k$ is the stiffness of the kth layer and t_k is the thickness of the kth layer.

The strain-curvature **coupling stiffness** matrix $[B]$:

$$[B] = \frac{1}{2}\sum_{k=1}^{N} \left(\overline{C}_{ij}\right)_k \left(z_k^2 - z_{k-1}^2\right) = \sum_{k=1}^{N} \left(\overline{C}_{ij}\right)_k t_k \overline{z}_k$$

$$= \begin{matrix} 0 & 0 & 0 \\ 0 & 0 & 0 \\ 0 & 0 & 0 \end{matrix} \quad \text{Msi-mil\textasciicircum2}$$

where $\overline{z}_k$ is the distance from the mid-plan to the centroid of the kth layer.

The **bending stiffness** matrix $[D]$:

$$[D] = \frac{1}{3}\sum_{k=1}^{N} \left(\overline{C}_{ij}\right)_k \left(z_k^3 - z_{k-1}^3\right) = \sum_{k=1}^{N} \left(\overline{C}_{ij}\right)_k \left(t_k \overline{z}_k^2 + \frac{t_k^3}{12}\right)$$

$$= \begin{matrix} 1.560 \times 10^7 & 1.703 \times 10^6 & 6.21 \times 10^{-4} \\ 1.703 \times 10^6 & 1.158 \times 10^7 & 0.006672 \\ 6.21 \times 10^{-4} & 0.006672 & 3.415 \times 10^6 \end{matrix} \quad \text{Msi-mil\textasciicircum3}$$

LIST OF REFERENCES

[1]   U.S. Navy. (2012, Jan). "US Navy Fact File: Trident Fleet Ballistic Missile," [Online]. Available: http://www.navy.mil/navydata/fact_display.asp?cid=2200&tid=1400&ct=2.

[2]   Lockheed Martin. (2011, Dec). "Trident II D5 Fleet Ballistic Missile (FBM)." [Online]. Available: http://www.lockheedmartin.com/us/products/trident-ii-d5-fleet-ballistic-missile--fbm-.html

[3]   G. J. Refuto, "Background on US strategic nuclear warfare theory and weapon technology," in *Evolution of the US Sea–Based Nuclear Missile Deterrent: Warfighting Capabilities,* Bloomington, IN, Xlibris Corporation, 2011, ch. I, pp. 26–74.

[4]   Air Command and Space College, "Intercontinental Ballistic Missiles," in *AU–18 Space Primer*. Maxwell AFB, AL, Air University Press, 2009, ch. 18, p. 247.

[5]   M. Aiguier, F. Bretaudeau and D. Krob, *Complex System Design and Management*, Heidelburg: Springer-Verlag, 2010.

[6]   Strategic System Programs. (2012, Jan). "FBM Weapon System 101—The Missiles." [Online]. Available: http://www.ssp.navy.mil/fb101/themissiles.shtml

[7]   Global Security.org. (2012, Feb). "Trident II D–5 Fleet Ballistic Missile–Recent Developments." [Online]. Available: http://www.globalsecurity.org/wmd/systems/d-5-recent.htm

[8]   O. O. Ochoa and J. N. Reddy, *Finite Element Analysis of Composite Laminates*, The Netherlands: Kluwer Academic Publishers, 1992.

[9]   J. N. Reddy and A. Miravete, *Practical Analysis of Composite Laminates*, Boca Raton, FL: CRC Press, Inc., 1995.

[10]   A. Moropoulou, A. Bakolas, and S. Anagnostopoulou. (2005, Feb.). Composite materials in ancient structures in *Cement and Concrete Composites*. [Online]. *27(2)*, pp. 295–300. Available: http://www.sciencedirect.com/science/article/pii/S0958946504000356

[11]   M. A. Meyers and K. K. Chawla, "Elasticity and Viscoelasticity," in *Mechanical Behavior of Materials*, 2nd ed. New York: Cambridge Univ. Press, 2009, ch.2, pp. 72–160.

[12]   J. C. Halpin, *Revised Primer on Composite Materials: Analysis*, Lancaster, PA: Technomic Publishing Company, Inc., 1984.

[13]   *Wood Handbook—Wood as an Engineering Material,* U.S. Department of Agriculture, Forest Service, Forest Products Laboratory, Madison, WI, Gen. Tech. Rep. FPL–GTR–113, 1999.

[14]   The Aviation Zone. (2012, Feb). Hughes HK–1 (H–4) "Spruce Goose." [Online]. Available: http://www.theaviationzone.com/factsheets/hk1.asp

[15]   D. S. Cairns and L. A. Wood, "ME 463 Design, Analysis, and Manufacturing Project," ME463 Design, Analysis, and Manufacturing Project, Mech. and Ind. Eng. Dept., Montana State Univ., Bozeman, MT, Fall Semester, 2009.

[16]   Naval Air Engineering Center, *Cloth, Glass, Finished, for Resin Laminates with Amendment 1*, MIL–C–9084C, Eng. and Specification Standards Dept., Code 93, Lakehurst, NJ, 9 Jun 1970.

[17]   ASTM International, *Standard Test Method for Structural Panels in Tension*, ASTM Standard D3500–90, West Conshohocken, PA, 1990 (Reapproved 2009).

[18]   ASTM International, *Standard Test Method for Wood–based Structural Panels in Compression*, ASTM Standard D3501–05a, West Conshohocken, PA, 2005 (Reapproved 2011).

[19]   eFunda: The Ultimate Online Reference for Engineers. (2012, Jan). [ABD] Calculator: Layout. [Online]. Available: http://www.efunda.com/formulae/solid_mechanics/composites/calc_ufrp_abd_matl.cfm.

[20]   Global Security.org. (2012, Feb). Trident II D–5 Fleet Ballistic Missile–Recent Developments. [Online]. Available: http://www.globalsecurity.org/wmd/systems/d-5-recent.htm

[21]   Matweb. (2012, Jan). Material Property Data–American Sitka Spruce Wood. [Online]. Available: http://www.matweb.com/search/DataSheet.aspx?MatGUID=1e56abdf98904f2ca53bff4bd1250cab

[22]   Matweb. (2012, Jan). Material Property Data–E–Glass Fiber, Generic. [Online]. Available: http://www.matweb.com/search/DataSheet.aspx?MatGUID=d9c18047c49147a2a7c0b0bb1743e812&ckck=1

INITIAL DISTRIBUTION LIST

1.   Defense Technical Information Center
      Ft. Belvoir, Virginia

2.   Dudley Knox Library
      Naval Postgraduate School
      Monterey, California